HHS Public Access

Author manuscript

*Cancer Discov*. Author manuscript; available in PMC 2020 July 01.

Published in final edited form as:

*Cancer Discov*. 2020 January ; 10(1): 142–157. doi:10.1158/2159-8290.CD-19-0529.

# ID1 mediates escape from TGF-β tumor suppression in pancreatic cancer

**Yun-Han Huang**[1,2,3], **Jing Hu**[1], **Fei Chen**[1], **Nicolas Lecomte**[4], **Harihar Basnet**[1], **Charles J. David**[1,10], **Matthew D. Witkin**[5], **Peter J. Allen**[6], **Steven D. Leach**[4,6,7,9], **Travis J. Hollmann**[7,8], **Christine A. Iacobuzio-Donahue**[4,7,8], **Joan Massagué**[1,*]

[1]Cancer Biology and Genetics Program, Sloan Kettering Institute, Memorial Sloan Kettering Cancer Center, New York, NY 10065

[2]Weill Cornell/Sloan Kettering/Rockefeller Tri-Institutional MD-PhD Program, New York, NY 10065

[3]Gerstner Sloan Kettering Graduate School of Biomedical Sciences, New York, NY 10065

[4]The David M. Rubinstein Center for Pancreatic Cancer Research, Memorial Sloan Kettering Cancer Center, New York, NY 10065

[5]Center for Epigenetics Research, Memorial Sloan Kettering Cancer Center, New York, NY 10065

[6]Department of Surgery, Memorial Sloan Kettering Cancer Center, New York, NY 10065

[7]Department of Pathology, Memorial Sloan Kettering Cancer Center, New York, NY 10065

[8]Human Oncology and Pathogenesis Program, Memorial Sloan Kettering Cancer Center, New York, NY 10065

[9]Present address: Department of Molecular and Systems Biology, Dartmouth Geisel School of Medicine, 1 Rope Ferry Road, Hanover, NH 03755-1404

[10]Present address: Tsinghua University School of Medicine, Department of Basic Sciences, Medical Sciences Building D106, Haidian District, Beijing, China, 100084

## Abstract

TGF-β is an important tumor suppressor in pancreatic ductal adenocarcinoma (PDA), yet inactivation of TGF-β pathway components occurs in only half of PDA cases. TGF-β cooperates with oncogenic RAS signaling to trigger epithelial-mesenchymal transition (EMT) in pre-malignant pancreatic epithelial progenitors, which is coupled to apoptosis owing to an imbalance of SOX4 and KLF5 transcription factors. We report that PDAs that develop with the TGF-β pathway intact avert this apoptotic effect via Inhibitor of Differentiation 1 (ID1). *ID1* family members are expressed in PDA progenitor cells and are components of a set of core transcriptional

[*]**Correspondence**: Joan Massagué, PhD, Box 116, Memorial Sloan Kettering Cancer Center, 1275 York Avenue, New York, NY 10065 USA, Phone: 646-888-2044, j-massague@ski.mskcc.org.

Author contributions

Conceptualization, J.M. and Y.H.; Methodology, Y.H., F.C., T.J.H.; Software, Y.H; Validation: C.I.D.; Formal Analysis, Y.H.; Investigation, Y.H., J.H., F.C., N.L., H.B., M.D.W, C.D., T.H.; Resources, J.M., C.I.D., P.A., S.L.; Data Curation, Y.H.; Writing – Original Draft, Y.H.; Writing – Review and Editing – J.M., Y.H., J.H.; Visualization, Y.H., F.C.; Supervision, J.M.; Funding Acquisition, J.M. and Y.H.

**Declaration of Interests**: J.M. is a science advisor and holds stock of Scholar Rock.

regulators shared by PDAs. PDA progression selects against TGF-β-mediated repression of *ID1*. The sustained expression of ID1 uncouples EMT from apoptosis in PDA progenitors. AKT signaling and mechanisms linked to low-frequency genetic events converge on *ID1* to preserve its expression in PDA. Our results identify ID1 as a crucial node and potential therapeutic target in PDA.

**Keywords**

TGF-β; pancreatic cancer; ID1; tumor suppression; EMT

## Introduction

Transfroming growth factor β (TGF-β) signaling mediates tumor suppressive or tumor progressive effects depending on the developmental context of a cancer cell (1). TGF-β causes apoptosis in premalignant cells that harbor RAS oncogenes (2,3). Some tumors develop with genetic inactivation of this pathway. However, a majority of tumors retain a functionally intact TGF-β pathway, somehow eliminating the tumor suppressive effect of TGF-β while benefiting from its invasive and immunosuppressive effects (1,4).

Pancreatic ductal adenocarcinoma (PDA), which has the highest incidence of TGF-β pathway mutations in cancer, is a paradigmatic example of this phenomenon. In normal pancreatic progenitors, the transcription factors KLF5 and SOX4 cooperatively impose an epithelial phenotype. Mutational activation of KRAS, a nearly universal tumor-initiating event in PDA, causes TGF-β to induce expression of the EMT transcription factor SNAIL, which represses KLF5 expression. As cells undergo a SNAIL-driven EMT in this dysregulated, KLF5-depleted context, SOX4 triggers a phenotype checkpoint by activating pro-apoptotic genes and cell death (3). TGF-β pathway inactivation, most frequently by mutation of *SMAD4*, occurs in one half of PDA cases. How the other half of PDAs retain an intact TGF-β pathway yet avert the pro-apoptotic effects remains an open question.

Genomic analysis of PDAs has revealed three other frequently mutated genes –*KRAS*, *CDKN2A* and *TP53*– in addition to *SMAD4* (5). Mutations in these three genes are not mutually exclusive with *SMAD4* mutations. Beyond these genetic alterations, PDAs present a long series of low frequency mutated genes (5). Given that no single, high-frequency genetic alteration has emerged as mutually exclusive to TGF-β pathway inactivation, we postulated that multiple alterations may converge on a common regulatory node that is critical to escape from tumor suppression in PDAs with an intact TGF-β pathway. Identifying this regulatory node would provide a potential therapeutic target in PDA.

To investigate this hypothesis, we focused on the analysis of dominant transcriptional networks in PDAs. Transcriptional dysregulation is a common feature of emerging tumors, reflecting adaptation to genetic alterations in cancer cells and inputs from the tumor microenvironment. Using this approach, we found that cancer cells from PDA tumors that develop with an active TGF-β pathway avert apoptosis by transcriptional dysregulation of ID1, an inhibitor of progenitor cell differentiation (6). Transcriptional induction of ID1 uncouples TGF-β-induced EMT from apoptosis. The dysregulation of ID1 expression results

from a diverse set of alterations, including PI3K-AKT signaling pathway mutations. ID1 thus emerges as a target of interest in pancreatic cancer.

## Results

### TGF-β signaling is active in half of pancreatic cancers

TGF-β signals through the paired receptor kinases TGFBR1 and TGFBR2 to phosphorylate SMAD2 and SMAD3 transcription factors, which associate with SMAD4 to activate target genes (Figure 1A) (1). *SMAD4* is inactivated in 38–43% of human PDAs, and the full set of TGF-β pathway core components collectively are inactivated in approximately 53% of PDAs (Supplementary Fig. S1A). To determine whether PDAs lacking mutations in these components retain a functional TGF-β pathway, we assayed 12 human PDA organoids for responsiveness to TGF-β. Activating *KRAS* mutations (G12D, G12V, or Q61H) were detected in all of the organoids, deleterious *TP53* mutations were identified in 8/12, and deleterious *TGFBR2* mutations in 4/12, reflecting the mutational spectrum of PDAs (Supplementary Table S1). Using induction of the common TGF-β target gene *SMAD7* as a readout, we found that six PDA organoids showed a weak increase (<3-fold; organoids HT22, HT33 and NL5) or no increase in *SMAD7* mRNA levels by TGF-β (HT30, HT42 and LMCB3) whereas the other six showed a 5- to 40-fold increase (Figure 1A). We designate these as “TGF-β-inactive” or “TGF-β-active” organoids. Since the functional transcriptional unit of TGF-β signaling is a trimer of receptor-phosphorylated SMAD2/3 with SMAD4, we determined by immunoblotting whether the organoids expressed SMAD4 and phosho-SMAD2 (pSMAD2) in response to TGF-β. Three of the TGF-β-inactive organoids (HT30, HT33, HT42) exhibited low levels of pSMAD2, consistent with receptor inactivation. HT30 has a *TGFBR2* N179Ifs*10 mutation, HT33 a *TGFBR2* P154Afs*3 mutation, and HT42 a *TGFBR2* R485H mutation. The other TGF-β-inactive organoids showed low levels of SMAD4. All TGF-β-active organoids stained positive for pSMAD2 and SMAD4 (Supplementary Fig. S1B), suggesting that a subset of PDAs retain a functionally intact TGF-β pathway.

To investigate this point in tissue samples, we stained for pSMAD2 in a tissue microarray of 130 human PDAs of which 69% were SMAD4-positive (7). Five percent of samples were negative for pSMAD2 in the tumor cells but were positive in the tumor stroma (Figure 1B–C), congruent with the frequency of genetic TGF-β receptor inactivation. 63% of the samples were positive for both pSMAD2 and SMAD4, suggesting the presence of TGF-β signaling components in the cancer cells of these tumors (Figure 1B–C). Mouse PDAs (8) showed pSMAD2 staining regardless of whether the tumors expressed wild type SMAD4 or not (Supplementary Fig. S1C). These results suggest that a large subset of PDA retains a functional TGF-β pathway and are exposed to TGF-β in the tumor microenvironment.

### Tumor suppressive TGF-β signaling alters a PDA transcriptional network

Progenitor cells are characterized by the expression of dominant transcription factors that specify the lineage and developmental stage of the cells. We decided to test the hypothesis that PDAs developing with either active or inactive TGF-β pathway achieve a common carcinoma stage end-point characterized by a particular transcriptional network. We

performed principal component analysis (PCA) of gene expression datasets from 225 cases of PDA, normal pancreas, and pancreatic neuroendocrine tumors (PNET) (9,10). PCA based on the top 5 transcription factors expressed within at least one case (53 total, Figure 1D, Supplementary Fig. S1D) showed separation of normal, PDA, and PNET samples. This separation was similar to that of PCA using a full list of expressed transcription factors (Supplementary Fig. S1E). The same analysis was applied to a second, independent PDA gene expression dataset (5) with similar results (Supplementary Fig. S1F). Notably, PDA cases with wild type or mutant TGF-β pathway components clustered together (Figure 1D), suggesting that PDA evolution selects for similar transcription factor networks regardless of the genetic integrity of the TGF-β pathway.

Of the transcription factors highly expressed in normal tissue, RBPJL, BHLHA15/MIST1 and NR5A2 are crucial in pancreatic specification and development of the acinar lineage, which is the putative cell of origin of PDA (11–13). In PNET, the highly expressed transcription factors correspond to the endocrine lineage: ISL1, MAFB, NKX2.2, PAX6 and ST18 (14–17). In PDA, the highly expressed transcription factors include AHR, HMGB2, ID1, KLF5 and PPARG, which play roles in epithelial progenitor specification and transformation (6,18–20). The expression level of the top five transcription factors was sufficient to separate normal samples from PDA samples by unsupervised hierarchical clustering (Figure 1E). In an independent dataset (21), these factors were enriched in PDAs of both the classical and the basal subtypes (Supplementary Fig. S1G), as well as in both primary and metastatic tumors (Supplementary Fig. S1H), suggesting that these five genes define a basic PDA transcriptional network.

To investigate the effect of TGF-β on the expression of the five PDA-associated transcription factors in a tumor suppressive context, we transduced a SMAD4 vector in cancer cells derived from mouse $Kras^{G12D}$;$Cdkn2a^{-/-}$;$Smad4^{-/-}$ PDA tumors (8), which restores the apoptotic effect of TGF-β (3). Notably, treatment of the SMAD4-restored PDA cells with TGF-β for 12 h, compared to treatment with SB505124 (a TGFBR1 kinase inhibitor used to suppress endogenous TGF-β activity), decreased the expression of the five transcription factors enriched in PDA, as determined by full transcriptome mRNA sequencing (RNA-seq) (Figure 1F). The effect was confirmed in a second mouse PDA cell line and two human PDA cell lines (Figure 1G). The effect was particularly pronounced with *Id1 and Pparg*, and was accompanied by induction of *Snai1*, encoding SNAIL (Figure 1H) (3), and expression of EMT and apoptosis signatures based on gene set enrichment analysis (GSEA) (Figure 1I). Thus, the PDA core transcription network is repressed in the context of a TGF-β tumor suppressive response.

## ID1 expression in pancreatic epithelial progenitors

ID1 was of particular interest because of the known role of the ID family members (ID1–4) in the negative regulation of cell differentiation (6). ID1–4 expression is high in progenitor cells and low in more differentiated cells. ID proteins lack a DNA binding domain and function by sequestering basic helix-loop-helix (bHLH) E-proteins to prevent their dimerization with differentiation bHLH transcription factors. TGF-β represses *ID1–3* in

epithelial progenitors (22) and induces *ID1* expression in breast cancer and glioblastoma cells (23–25).

To better understand the role of ID1 in PDA, we stained for ID1 in a panel of human pancreatic tissues including normal pancreas, pancreatic intraepithelial neoplasias, primary PDAs, and PDA metastases. Epithelial cells stained positive for ID1 within PDA samples (Figure 2A). Of the 30 cases of human PDA that we examined, 24 (80%), including 14 of 16 SMAD4+ tumors and 10 of 14 of Smad4-negative tumors, exhibited cancer cells with nuclear ID1 staining. In normal human pancreatic tissues from 6 patients who had no signs of pancreatic disease, nuclear ID1 staining was observed in endothelial cells and in fewer than 1% of epithelial cells (Figure 2A).

We devised a four-color multiplex immunohistochemical staining method to examine ID1, KLF5 and SOX4 and cytokeratins together in PDA samples surgically resected from 6 patients of known SMAD4 status (Figure 2B, Supplementary Table S2). ID1+,KLF5+,SOX4+ cells constituted only a small proportion (mean 5.5%, range 0.2% to 13.2%) of the cancer cell population in these samples (Figure 2C, Supplementary Table S1). 55.9% of the carcinoma cells expressed none or only one of these progenitor markers. Notably, ID1-,KLF5-,SOX4+ cells were less abundant (mean 3.8%, range 0.6%−12.3%) than ID1+,KLF5-,SOX4+ cells (mean 7.0%, range 4.8%−11.8%). Among SMAD4+ samples (samples 2, 4, 6; Supplementary Table S1), ID1-,KLF5-,SOX4+ cells were even less abundant (mean 1.1%, range 0.6%−2.1%) compared to ID1+,KLF5-,SOX4+ cells (mean 7.5%, range 4.9%−10.2%). ID1-,KLF5-,SOX4+ cells were the least abundant population overall in the sample set as well as in individual cases, except for one case of poorly differentiated SMAD4-negative PDA which had large ID1+ cell populations compared to the other cases (Supplementary Table S1). These results are consistent with our hypothesis that SOX4+ cells lacking ID1 and KLF5 expression survive poorly, particularly in SMAD4+ PDAs.

Like the human PDAs, 3/3 normal mouse pancreata were negative for ID1 whereas 6/6 PDAs from different autochthonous and orthotopic mouse models ($Kras^{G12D}$;$Cdkn2a^{-/-}$ or $Kras^{G12D}$;$Trp53^{R172H}$ or $Kras^{G12D}$;$Cdkn2a^{-/-}$;$Smad4^{-/-}$) showed ID1 staining in 46%−47% of cancer cells regardless of *Smad4* status (Supplementary Fig. S2A,B). PDX1 (pancreatic and duodenal homeobox 1) is a transcription factor of pancreatic progenitors (26). ID1+ cells constitute a subset of PDX1+ cells in orthotopic pancreatic tumors (Supplementary Fig. S2C,D). Amylase, a marker of mature pancreatic acinar cells, was mutually exclusive with ID1 immunofluorescence (Supplementary Fig. S2D). In freshly dissociated $Kras^{G12D}$;$Cdkn2a^{-/-}$;$Smad4^{-/-}$ orthotopic tumors the ID1+ population is also enriched for cells surface markers (CXCR4, SSEA4, CD44, CD24) previously associated with pancreatic cancer stem cells (Supplementary Fig. S2E,F) (27–29).

To recapitulate the heterogeneity in ID1 expression observed in pancreatic tumors we created a knock-in green fluorescent protein (*GFP*) reporter at the endogenous *Id1* locus in mouse $Kras^{G12D}$;$Cdkn2a^{-/-}$;$Smad4^{-/-}$ PDA cells (ID1-GFP cells) (Figure 2D,E, Supplementary Fig. S2G,H). $GFP^{high}$ cells isolated by FACS from these populations grew better in a surrogate growth assay for stem-like cancer cells in which the cells grow as

spheroid colonies ("oncospheres") in low-attachment plates with limited growth factors (28) (Figure 2F). The transcriptional signature of pancreatic stem cells is not well defined. However, the GFP$^{high}$ cells expressed signatures associated with breast cancer progenitors and intestinal stem cells, as determined by RNA-seq and GSEA (Supplementary Fig. S2I) (30,31). In contrast, GFP$^{low}$ cells expressed signatures of pancreatic epithelial differentiation (Supplementary Fig. S2J). The data indicate that ID1 is expressed in a large population of PDA cells including progenitor cells.

## ID1 family promotes tumorigenic activity in pancreatic progenitors

*ID* genes are frequently co-expressed and have overlapping functions (6). *ID2* and *ID3* were enriched in human PDAs albeit less than was *ID1* (Supplementary Fig. S2K). Of six human PDA samples in which nuclear ID1 was not detected, three showed nuclear stainig for ID2, one for ID3, and two for ID2 and ID3 (Supplementary Fig. S2L,M). shRNA-mediated knockdown of *Id1* stimulated the expression of *Id2* in *Kras$^{G12D}$;Cdkn2a$^{-/-}$;Smad4$^{-/-}$* PDA cells, and *Id2* knockdown stimulated that of *Id1 and Id3* (Supplementary Fig. S2N). Knockdown of *Id1* decreased the spheroid-forming ability of these PDA cells, and additional knockdown of *Id2* and *Id3* further decreased spheroid growth (Figure 2G). Thus, ID1 ID2 and ID3 are expressed in a compensatory manner and show a partial functional overlap in PDA cells.

We orthotopically implanted *Kras$^{G12D}$;Cdkn2a$^{-/-}$;Smad4$^{-/-}$* mouse pancreatic cells with doxycycline-inducible expression of *Id1~3* shRNAs and tumor growth was tracked by bioluminescence imaging (BLI) of a transduced firefly luciferase gene. The knockdown of *Id1* alone decreased tumorigenic potential by approximately 10-fold (Supplementary Fig. S2O). The knockdown of *Id1~3* further decreased this potential (Figure 2H, Supplementary Fig. S2P), and prolonged survival of the tumor-bearing mice (Figure 2I), compared to doxycycline treatment of tumors expressing a control shRNA (shRen). ID1 immunostaining was present in the late-emerging *Id1~3* shRNA tumors, indicating tumor formation by cells that escaped *Id1* depletion (Supplementary Fig. S2Q).

To determine if the requirement for the ID proteins is retained in an established tumor, we orthotopically implanted PDA cells harboring inducible *Id1–3* shRNAs, allowed the tumors to grow for 3 weeks, and then randomized the mice into matched bioluminescence groups for treatment with doxycycline. Doxycycline-treated mice had lower tumor burdens and longer survival (Figure 2J,K). *Id1–3* shRNAs also decreased the formation of orthotopic tumors by a cell line derived from a *Kras$^{G12D}$;Cdkn2a$^{-/-}$* mouse PDA (Figure 2L,M). These observations suggest that the ID family supports the tumorigenic potential of PDA cells.

## ID1 downregulation is associated with apoptosis

The emergence of ID1 as a top PDA transcriptional network component, and its tumorigenic activity in PDA progenitor cells led us to investigate whether ID1 downregulation by TGF-β is deleterious to these cells. To simulate the premalignant, TGF-β-sensitive state, we restored SMAD4 expression in *Kras$^{G12D}$;Cdkn2a$^{-/-}$;Smad4$^{-/-}$* mouse PDA cells and human SMAD4-null PDAs. Additionally, we derived pre-malignant cells from *Kras$^{G12D}$;Cdkn2a$^{-/-}$* mouse pancreata. We then queried the TGF-β response of cells from these various models

(Figure 3A). TGF-β inhibited *Id1* expression and induced *Snai1* expression (Figure 3B) and apoptosis (Figure 3C) in organoids derived from $Kras^{G12D}$;$Cdkn2a^{-/-}$ mouse pancreata. RNA-seq data from the SMAD4-restored mouse PDA cells showed that TGF-β also decreased the expression of *Id2* and *Id3* (Figure 3D), in association with the induction of *Snai1* (refer to Figure 1G) and cleaved caspase 3 (Figure 3E). The decrease in *Id1–3* expression was accompanied by an increase in protein binding to an E-box motif oligonucleotide in electrophoretic mobility shift assay (EMSA) (Supplementary Fig. S3A), consistent with a decrease in ID activity in these cells.

In SMAD4-restored mouse PDA cells containing an endogenous ID1-GFP reporter, the sorted $GFP^{high}$ cells showed ID1-GFP downregulation by TGF-β (Figure 3F,G), which was accompanied by induction of *Snai1* (Supplementary Fig. S3B) and apoptosis (Figure 3H, Supplementary Fig. S3C). In contrast, the $GFP^{low}$ counterparts did not undergo apoptosis in response to TGF-β (Figure 3H, Supplementary Fig. S3C), although they showed SMAD2 phosphorylation and *Snai1* expression in response to TGF-β (Figure 3I,J). These ID1-$GFP^{low}$ cells express less SOX4 than the ID1-$GFP^{high}$ cells (Supplementary Fig. S3D), and high expression of SOX4 enables TGF-β-mediated apoptosis (3). Expression of SOX4 from an inducible promoter increased TGF-β-mediated apoptosis in ID1-$GFP^{low}$ cells (Figure 3K, Supplementary Fig. S3E). These results suggest that TGF-β-induced ID1 downregulation and apoptosis are specific responses of $ID1^{high}$ PDA progenitors whereas the more differentiated progeny is protected from apoptosis by a decrease in SOX4 expression.

## Dysregulated ID1 expression in PDAs with a functional TGF-β pathway

In contrast to SMAD4-restored PDA cells, cells derived from PDAs that developed with a functional TGF-β pathway were resistant to TGF-β-induced apoptosis (Figure 4A–D) and, notably, retained *ID1* expression in the presence of TGF-β (Figure 4E). TGF-β increased *ID1* expression in human PDA organoids that had a functional TGF-β pathway (Figure 4F), and the extent of this induction tracked with that of *SMAD7* across the cohort (refer to Figure 1A).

To recapitulate this phenomenon in cells derived from the same genetic background, we cultured SMAD4-restored mouse PDA cells (S4 cells) for 3 weeks with TGF-β and selected for cells resistant to the pro-apoptotic effect of TGF-β (Figure 4G). This selection protocol was done in the presence of the allosteric AKT inhibitor MK2206, which synergizes with TGF-β in the induction of apoptosis in PDA cells (3). The cells that we derived (S4.1 cells) were resistant to the pro-apoptotic effects of TGF-β (Figures 4H, Supplementary Fig. S4A) but still induced *Smad7* expression (Figure 4I) and underwent an EMT in response to TGF-β (Supplementary Fig. S4B). Notably, whereas TGF-β treatment downregulated *Id1* in the S4 parental population, it increased *Id1* expression in S4.1 cells (Figures 4I–J) and in two other independent populations (S4.2 and S4.3) isolated with the same protocol (Supplementary Fig. S4C). Besides *Id1*, only four other genes were differentially regulated by TGF-β by more than 4-fold: *Id3*, *Fam167a*, *Trib3*, and *Chac1* (Figure 4I). *Id2* was differentially regulated by TGF-β but less than 4-fold. RNA polymerase II (RNAPII) ChIP-seq analysis in S4 and S4.1 cells showed RNAPII already occupied the promoter of *Id1* under basal conditions, and TGF-β decreased the occupancy in S4 cells but increased it in S4.1 cells

(Supplementary Fig. S4D). *Id1–3* knockdown in S4.1 cells rescued the TGF-β-induced apoptosis (Figure 4K).

TGF-β had similar effects on SMAD2/3 and SMAD1/5 phosphorylation in S4 and S4.1 cells (Supplementary Fig. S4E), ruling out a switch in SMAD signaling (32) as an explanation for the induction of *Id1* in these cells. Functional annotation of the genes differentially expressed between the S4 and S4.1 cells (average expression >10 readcounts, fold change >2, $p<0.05$) showed that the top enriched pathways were related to small molecule metabolism (Supplementary Fig. S4F). The common genes between these pathways were all UDP glucuronosyltransferases (UGTs), which are key enzymes for the inactivation of polycyclic compounds, including MK2206 (33). Several UGTs were up-regulated in the S4.1 cells (Supplementary Fig. S4G). We generated a signature of differentially expressed genes (average expression > 10 readcounts, fold change > 4, $p<0.05$) in S4 cells treated with 2.5 μM MK2206 for 16h. The MK2206 gene signature was decreased in the S4.1 cells relative to the S4 cells treated under these conditions (Supplementary Fig. S4H), consistent with a low effectiveness of MK2206 in the S4.1 cells. Collectively, these results indicate that human and mouse PDA cells that retain an active TGF-β pathway do not downregulate ID1 expression in response to TGF-β.

## ID1 uncouples TGF-β-induced EMT from apoptosis

Next, we tested the hypothesis that loss of TGF-β-mediated ID1 repression protects PDA progenitors from pro-apoptotic TGF-β effects. Enforced expression of *Id1* from an inducible promoter in SMAD4-restored mouse PDA cells (Figure 5A) inhibited the apoptotic effect of TGF-β (Figure 5B). When these cells were implanted into mice with caerulein-induced acute pancreatitis, which mimics the TGF-β-rich microenvironment of the premalignant pancreas, enforced expression of *Id1* conferred resistant to apoptosis (Figure 5C) and promoted tumor growth (Figure 5D).

The enforced expression of *Id1* caused few changes in basal gene expression (average readcounts >10, fold change >2, $p<0.05$, Supplementary Fig. S5A) and in TGF-β gene responses (Figure 5E), but decreased the ability of TGF-β to induce several genes with described pro-apoptotic actvities: *Fbxo32, Rnf152, Bmf, Ndrg1, and Errfi1*. Using qRT-PCR we confirmed that enforced expression of *Id1* decreased the induction of *Fbxo32* and *Rnf152* by TGF-β without affecting the induction of *Snail1* or *Smad7* (Supplementary Fig. S5B). *Id1* expression did not interfere with the enrichment for an EMT gene signature (Figure 5F), the induction of EMT effectors (*Snai1*, *Zeb1*, *Zeb2* and *Cdh2*), or the downregulation of Snail-repressed genes *Cdh1* (E-cadherin), *Klf5* and *Krt19* (cytokeratin 19) in response to TGF-β (Figure 5A,G). Under prolonged (72 h) treatment with TGF-β SMAD4-restored cells with enforced *Id1* expression survived with a mesenchymal phenotype (Figure 5H). These results suggest that TGF-β repression of ID1 is necessary for the apoptotic effect whereas sustained expression of ID1 decouples TGF-β-induced EMT from apoptosis.

SMAD binding motifs and E-box binding motifs were enriched within accessible chromatin regions near the ID1-inhibited genes, as detected by ATAC-seq (Supplementary Fig. S5C). SMAD2/3 bound to a subset of these chromatin regions in the presence of TGF-β

(Supplementary Fig. S5D), including near the ID1-regulated proapoptotic genes (Supplementary Fig. S5E). Focusing on the accessible chromatin regions of *Fbxo32* and *Rnf152*, we confirmed the presence of SMAD and E-protein binding sequences in these regions, (Supplementary Fig. S5E). TGF-β induced the binding of SMAD2/3 to these regions, as determined by ChIP-PCR (Supplementary Fig. S5F). The E-proteins E12/E47 were also bound to these enhancers (Supplementary Fig. S5G). ID1 expression caused a decrease in E12/E47 binding without significantly affecting the binding of SMAD2/3 (Supplementary Fig. S5F,G). These results are consistent with the mode of action of ID proteins, which is by preventing the binding of E-proteins to DNA (6).

## Dysregulation of ID1 repression as a nodal point

The observed switch of the ID1 response to TGF-β from repression to activation provides a mechanism for tumor progression by PDAs that develop with a functional SMAD pathway. Given the highly recurrent genetic alterations in PDA (i.e. *KRAS*, *TP53*, *CDKN2A*) are not mutually exclusive to TGF-β pathway alterations (refer to Supplementary Fig. S1A), we postulated that low-frequency alterations in multiple factors achieve the same common end of preventing the repression of ID1 by TGF-β. We performed a genome-wide CRISPR/Cas9 screen to identify factors that enable ID1 repression by TGF-β. We transduced SMAD4-restored mouse PDA cells containing the endogenous ID1-GFP reporter with the Gecko_v2 genome-wide library containing 123,411 sgRNAs (34,35) and treated the cells with TGF-β or SB505124 for 36 h. To select cells that bypassed *Id1* repression by TGF-β, we sorted for ID1-GFP$^{high}$ cells, and repeated this procedure three times to improve the stringency of the screen (Figure 6A).

sgRNAs targeting TGF-β pathway components were enriched in the samples treated with TGF-β (Figures 6B, Supplementary Fig. S6A), providing a positive control for the screen. In addition, Biocarta pathway analysis of the data identified PI3K/AKT-related pathway components (AKT, EGF, IGF1, IGF1R, INSULIN, PTEN, HER2, MTOR, NGF) as being depleted in the TGF-β-treated samples (Figure 6C). Analysis of genetic events in the MSK-IMPACT dataset (36) for alterations occurring with mutual exclusivity tendencies to TGF-β pathway inactivation demonstrated concordant depletion of PI3K/AKT-related pathways (Figure 6D).

## PI3K/AKT input into ID1 regulation

Several PI3K/AKT activating events including *INSR* and *AKT2* amplification and *PIK3CA* and *PTEN* mutation occur in a subset of PDA with intact TGF-β pathway (Supplementary Fig. S6B). Allowing AKT signaling, either by excluding MK2206 from the media or by expressing the MK2206-resistant mutants AKT1(W80A) and AKT2(W80A) (37), prevented TGF-β-mediated *Id1* repression and apoptosis in SMAD4-restored cells (Figures 7A–B, Supplementary Fig. S7A), while still allowing TGF-β induction of *Snai1* and EMT (Figures 7C, Supplementary Fig. S7A). These results provided further evidence that PI3K/AKT activation selectively prevents TGF-β-mediated ID1 repression and decouples TGF-β-induced EMT from apoptosis in PDA cells.

Five regions of high accessibility (regions 1~5) were detected in the *Id1* locus in SMAD4-restored mouse PDA cells (Figure 7D). These regions were conserved in the *ID1* locus in human Panc1 PDA cells (Supplementary Fig. S7B). SMAD2/3 interacts with regions 1, 3 and 4 in SMAD4-restored mouse PDA cells in a TGF-β-dependent manner (Figure 7D). Region 1, which is located approximately 1 kb upstream of the transcription start site (TSS), is implicated in the downregulation of ID1 by TGF-β in other cells types (22,38). PI3K/AKT signaling upregulates ID1 expression by excluding the transcription factor FOXO3a from the nucleus (39). Indeed, FOXO1 and FOXO3a interacted with *Id1* regions 1 and 2 (Figure 7E). In pooled CRISPR/Cas9 modified cells, modification of Region 2 blocked the repression of ID1 by TGF-β, as did targeting of *Tgfbr2* (Figure 7F). Mouse PDA tissues demonstrated more extensive FOXO1 nuclear exclusion in $Kras^{G12D};Cdkn2a^{-/-}$ tumors than in $Kras^{G12D};Cdkn2a^{-/-},Smad4^{-/-}$ tumors, suggesting higher AKT signaling in the SMAD4+ tumors (Supplementary Fig. S7C). Some cells isolated from $Kras^{G12D};Cdkn2a^{-/-}$ PDAs were sensitive to TGF-β-induced apoptosis in the presence of AKT inhibition (Supplementary Fig. S7D). Collectively, these results suggest that PI3K/AKT activation constitutes one mechanism for the dysregulation of ID1 repression to evade TGF-β-mediated tumor suppression in PDA cells.

## Discussion

To survive the apoptotic effect of TGF-β during tumor formation, KRAS-mutant pancreatic progenitors must either genetically alter the TGF-β pathway or decouple it from apoptosis. Mutational inactivation of SMAD4 or TGF-β receptors eliminates TGF-β tumor suppressive responses in ~50% of human PDA cases. Our new findings identify an escape mechanism for the other cases by showing that ID1 decouples TGF-β-induced EMT from apoptosis in PDA cells (Figure 7G). A key finding of the current study is that transcriptional dysregulation of ID1 is a selected, common feature of PDAs, which imparts both progenitor-like characteristics to PDA cells and protects from TGF-β-induced apoptosis. We show that a combination of signaling inputs and genetic alterations contribute to the maintenance of high ID1 levels in PDAs. Other bHLH factors necessary in pancreatic development, including MIST1 and PTF1A, have tumor suppressive roles in the pancreas (40,41), and together with our observations, this suggests that a critical balance between inhibitory and activating bHLH factors controls pancreatic homeostasis.

TGF-β-induced apoptosis occurs in PDA progenitor stages that express SOX4 and KLF5 and depend on cooperation between these transcription factors for maintenance of their epithelial progenitor phenotype and survival (3). TGF-β and RAS signaling synergize to potently induce SNAIL expression, which triggers a phenotype checkpoint through a proapoptotic imbalance between SOX4 and KLF5. We now show that ID1 expression averts apoptosis in this context. More differentiated PDA cell progenies that express low levels of ID1 and SOX4 do not die in response to TGF-β, but these ID1/SOX4-low cells are also poorly tumorigenic. By uncoupling TGF-β signaling from apoptosis, ID1 allows PDA progenitors to retain EMT and other effects of TGF-β which provide tumors with selective advantages in immune evasion, invasion, and metastasis (1). The ability to uncouple the pro-apoptotic and EMT effects of TGF-β provides a framework for targeting specific features of this pathway.

The PI3K/AKT pathway emerged in our work as a signal for ID1 dysregulation. PI3K/AKT activating mutations are relatively rare in PDA compared to other tumor types. However, insulin signaling is particularly relevant in the pancreas, where blood flows through the insulin-synthesizing islets of Langerhans to the capillaries prior to supplying the pancreatic acini and ducts (42). Furthermore, several studies have connected high levels of circulating insulin with increased incidence of PDA and resistance to the pro-apoptotic effects of PI3K inhibition (43–45). AKT2 amplification and a microenvironment rich in insulin may potentiate PI3K/AKT signaling in the pancreas and contribute to the observation that receptor tyrosine kinase activation is necessary for PDA formation even in the presence of mutant KRAS (46,47). The tail of low-frequency genetic alterations that are exclusive of *SMAD4* mutations in genome-wide studies of PDA may contain additional mediators of ID1 dysregulation besides AKT pathway components.

Our analysis demonstrates that focusing on highly expressed transcriptional regulators yields commonalities in PDA. Our analysis using a rank-based, transcription factor-centered algorithm allowed us to identify factors that are key to integrating microenvironmental signals and genetic alterations to orchestrate cell fates and states. Transcription factors that are highly and differentially expressed frequently represent lineage dependencies and constitute promising therapeutic targets. Our findings suggest that PDAs of different subtypes possess common transcriptional dependencies, such as on ID1. Small molecule inhibitors of ID proteins have been reported (48). Based on the dependence of PDA cells on ID1, we predict that PDAs would be particularly sensitive to these inhibitors.

## METHODS

### Human subjects research

The study was conducted under Memorial Sloan-Kettering Cancer Center Institutional Review Board approval (MSKCC IRB 15–149 or 06–107) and all patients provided written informed consent prior to tissue acquisition. Normal pancreas and PDA samples were collected from patients undergoing routine surgical resection and as part of MSKCC's rapid autopsy program for paraffin embedding or organoid generation. Normal pancreatic samples were from six patients with tumors at distant sites (lung and brain) with no observed pathology in the pancreas.

### Animal experiments

Animal experiments were performed as approved by the MSKCC Institutional Animal Care and Use Committee. For orthotopic tumor models, 500 dissociated cells were implanted in 25 μL of Matrigel (Corning Matrigel GFR Membrane Matrix, #356231), injected through 31G syringes into the pancreata of 4-week old female FVB (JAX, FVB/NJ) or athymic nude mice (ENVIGO, Hsd: Athymic Nude-*Foxn1nu*). Mice were started on 2500 mg/kg doxycycline diet (ENVIGO, TD.07383 2014–2500-B, irradiated) after cell implantation for Tet-On shRNA experiments. Tumor growth was tracked weekly using bioluminescence (Goldbio Firefly D-Luciferin, potassium salt). Tumors were collected from genetic mouse models of PDA (*LSL-Kras*$^{G12D}$;*Cdkn2a*$^{fl/fl}$;*Smad4*$^{fl/fl}$ and *LSL-Kras*$^{G12D}$;*Cdkn2a*$^{fl/fl}$) for cell lines, organoid lines, and immunohistochemistry. Acute pancreatitis was induced by

caerulein injection with 8 hourly injections of 50 μg/kg on 2 consecutive days. For AKT inhibition, mice were dosed by oral gavage with 100 mg/kg MK2206 dissolved in Captisol as a carrier.

## Cell culture

Pancreatic organoids were generated as previously described (49) and maintained embedded in Matrigel with Advanced DMEM/F12 (Gibco, 12634–028) supplemented with B-27 (Life Technologies, 12587–010), HEPES (10 mM), 50% Wnt/R-spondin/Noggin-conditioned medium (ATCC, CRL-3276), Glutamax (Invitrogen, 2 mM), N-acetyl-cysteine (Sigma, 1 mM), nicotinamide (Sigma, 10 mM), epidermal growth factor (Peprotech, 50 ng/mL), gastrin (Sigma, 10 nM), fibroblast growth factor-10 (Peprotech, 100 ng/mL), A83–01 (Tocris, 0.5 μM) as previously described (49). Pancreatic spheroids were grown in Ultra Low Attachment Culture plates (Corning) in DMEM supplemented with Glutamax (2 mM) and heparin (5 μg/mL). All cell lines and organoids were maintained at 37°C and 5% $CO_2$.

Human pancreatic cancer cell lines BxPC3, MiaPaca2 and Panc1 were obtained from ATCC in 2012. Human pancreatic cancer cell line A21 was obtained in 2016 (50). The 806 and 906 *Kras*$^{G12D}$; *Cdkn2a*$^{-/-}$; *Smad4*$^{-/-}$ mouse PDA cell lines and the NB44 *Kras*$^{G12D}$; *Cdkn2a*$^{-/-}$; *Smad*$^{+/+}$ mouse PDA cell line were provided by N. Bardeesy in 2011 (8). The 4279 cell line was derived from a *Kras*$^{G12D}$; *Cdkn2a*$^{-/-}$; *Smad*$^{+/+}$ mouse PDA tumor in this lab. Pancreatic cell lines were maintained in high glucose DMEM supplemented with 10% FBS and 2 mM L-glutamine. Cell lines were authenticated by Western blot verification of expected genetic alterations or transcriptomic evaluation of appropriate gene expression. Cell lines were frozen in FBS with 10% DMSO and stored in liquid nitrogen indefinitely. Organoid lines were frozen in organoid growth media with 50% FBS and 10% DMSO. Cell lines were used within 1 month of culture from cryopreserved stocks and were tested for mycoplasma contamination at the time of acquisition and cryopreservation. Organoids were used between passages 5 and 25, and were tested for mycoplasma contamination after use or 1–6 passages before use.

## Four-color immunohistochemical multiplex staining

Four μm sections obtained from tissue blocks were baked for 3 h at 62°C with deparafinization performed on the Leica Bond RX followed by 4 sequential rounds of staining, each round including a combined block with primary antibody (PerkinElmer antibody diluent/block ARD1001) followed by a corresponding secondary horseradish peroxidase (HRP)-conjugated polymer (PerkinElmer Opal polymer HRP Ms + Rb ARH1001). Each HRP-conjugated polymer induces the covalent binding of fluorophores to tissue using tyramide signal amplification. The covalent reaction was followed by heat induced stripping of the primary antibody in Perkin Elmer AR9 buffer (AR900250ML) for 20 min at 100°C before the next step in the sequence. The antibodies were sequentially stained in the following order: ID1 (BioCheck, 1:300), KLF5 (R&D Systems, 1:200), Sox4 (Abcam, 1:600) and kertain cocktail (PanCK (Dako, 1:200), CK7 (Abcam, 1:400) and CAM5.2 (Becton Dickinson, 1:150)). Following incubation of the KLF5 goat polyclonal primary antibody, detection was performed using a rabbit anti-goat secondary (Vector lab, 1:4,000) followed by the aforementioned PerkinElmer Opal polymer. After 4 sequential

rounds of staining, sections were stained with Hoechst 33342 (Invitrogen) to visualize nuclei and mounted with ProLong Gold antifade reagent mounting medium (Invitrogen).

### Chromatin immunoprecipitation (ChIP)

$10^7$ cells were collected for each ChIP sample. Cells were crosslinked at 37°C for 10 min with 1% formaldehyde, quenched with 125 mM glycine, washed with PBS, and sonicated in lysis buffer: 50 mM HEPES/KOH pH7.5, 140 mM NaCl, 0.1% Na-deoxycholate, 1% Triton X-100, 1 mM EDTA, complete protease inhibitor cocktail (Roche). Samples were incubated with 5 μg of anti-RNAPII (Abcam), anti-Smad2/3 (Cell Signaling), or anti-E12 (Santa Cruz) for overnight and washed 7 times with 20 mM Tris, pH7.9, 500 mM NaCl, 2 mM EDTA, 1% Triton X-100, 0.1% SDS. After one wash with Tris-EDTA (TE), DNA was eluted in TE+1% SDS for 1 h at 65°C, and reverse-crosslinked with RNAse A for 4 h and Proteinase K for 1 h at 65°C. DNA was purified using a PCR Purification Kit (Qiagen).

Libraries were prepared using the NEBNext ChIP-seq Library Prep Master Mix Set for Illumina (NEB, E6240L) and quality checked using Agilent Technologies 2200 TapeStation to determine fragment size and PicoGreen (Life Technologies/Invitrogen, P7589) to quantify concentration. Samples were pooled and submitted to New York Genome Center for single-end 50 bp sequencing using a HiSeq 2500.

### ATAC-seq

50,000 cells were collected and washed with 1mL of cold PBS, then 1mL of ice-cold ATAC Buffer (10mM Tris pH 7.4, 10mM NaCl, 3mM MgCl2). Cells were suspended in 50μL of ATAC Lysis Buffer (10mM Tris pH 7.4, 10mM NaCl, 3mM MgCl2, 0.1% NP-40 or IGEPAL-Ca630), incubated on ice for 2 min. 1mL of cold ATAC Buffer was added and nuclei were pelleted at 1500rpm for 10 min at 4°C in a bucket centrifuge. Nuclei were resuspended in 22.5μL of the supernatant and transferred to 2.5μL Tagmentation Enzyme (transposase) and 25μL of Tagmentation Buffer (Illumina Nextera DNA Sample Preparation Kit). Reaction was incubated at 37°C for 30 min. After tagmentation, SDS (final concentration of 0.2%) was added and sample was incubated at room temperature for 5 min before purifying with 2X Agencourt AMPure XP beads (Beckman Coulter A63881). Purified samples were eluted in 50μL of 0.1X Tris-EDTA.

Libraries were prepared with 50 μL sample + 55μL of NEBNext Q5 Hot Start HiFi PCR Master Mix (NEB, catalogue M0543L) and 5μL of primer mix using 25 μM of the Nextera primers (51). PCR amplification was performed as previously described for 12 cycles. Samples were purified with 1.5x AMPure XP beads. Concentration was measured using PicoGreen and median fragment size measured using the Agilent D1000 screentape on a Agilent Technologies 2200 TapeStation. Samples were sequenced (paired-end 50 bp) on a HiSeq 2500.

### CRISPR Screening

CRISPR screenings were performed as described (35). For the whole genome screen, the GeCKO v2 mouse whole genome library (Addgene Pooled Library 1000000049) was introduced into an 806-SMAD4pLVX-ID1GFP-Cas9Blast clone at 10% infection efficiency

and 200x representation. Cells were plated at $2\times10^6$ per plate in 2.5 μM MK2206 for 12 h and then treated with 2.5 μM SB505124 or 100 pM TGF-β for 36 h prior to collection for FACS. Between rounds of selection, cells were expanded in 15 cm plates and representation was kept at >200x.

### Data availability

All RNA-Seq, ChIP-Seq and ATAC-Seq data were deposited in the Gene Expression Omnibus database under accession number (GSE112940).

### Additional methods

Genetic knockins, knockouts, knockdowns and overexpression, immunoblotting, immunohistochemistry, immunofluorescence, flow cytometry, data analysis methods, oligonucleotide and antibody reagents are described in the Supplementary Merthods section.

## Supplementary Material

Refer to Web version on PubMed Central for supplementary material.

## Acknowledgements

We thank L. Cantley, A. Ventura, R. Benezra, R. Levine, E. Er, R. Koche, and K. Ganesh for thoughtful discussion of this project. We also thank Y. Li, J. Hampton, S.E. Kim, and M. Overholtzer for assistance with experiments. We gratefully acknowledge the support of the Marie-Josée and Henry R. Kravis Center for Molecular Oncology, the Molecular Diagnostics Service, the Center for Epigenetics Research, the Integrated Genomics Core, and the Flow Cytometry Core of MSKCC. Funding was provided by National Cancer Institute grants R01-CA34610 (JM), R35-CA220508 (CIA) and P30-CA008748 (MSKCC). Y.H. was supported by Medical Scientist Training Program grant T32-GM007739, and Predoctoral Fellowship F30-CA203238 from the National Cancer Institute.

**Financial support**: National Cancer Institute grants R01-CA34610 (JM) and P30-CA008748 (MSKCC), and Predoctoral Fellowship F30-CA203238 (YH). Medical Scientist Training Program grant T32-GM007739 (YH).

## Abbreviations

| | |
|---|---|
| **TGF- β** | transforming growth factor β |
| **PDA** | pancreatic ductal adenocarcinoma |
| **EMT** | epithelial-mesenchymal transition |
| **ID1** | inhibitor of differentiation 1 |
| **pSMAD2** | phospho-SMAD2 |
| **PCA** | principal component analysis |
| **PNET** | pancreatic neuroendocrine tumors |
| **RNA-seq** | mRNA sequencing |
| **GSEA** | gene set enrichment analysis |
| **Bhlh** | basic helix-loop-helix |

| | |
|---|---|
| **GFP** | green fluorescent protein |
| **EMSA** | electrophoretic mobility shift assay |

## Citations


1. David CJ, Massague J. Contextual determinants of TGFβ action in development, immunity and cancer. Nature Reviews Molecular Cell Biology 2018;164:1015–30.
2. Guasch G, Schober M, Pasolli HA, Conn EB, Polak L, Fuchs E. Loss of TGFbeta signaling destabilizes homeostasis and promotes squamous cell carcinomas in stratified epithelia. Cancer Cell 2007;12:313–27. [PubMed: 17936557]
3. David CJ, Huang YH, Chen M, Su J, Zou Y, Bardeesy N, et al. TGF-beta Tumor Suppression through a Lethal EMT. Cell 2016;164:1015–30. [PubMed: 26898331]
4. Batlle E, Massague J. Transforming Growth Factor-beta Signaling in Immunity and Cancer. Immunity 2019;50:924–40. [PubMed: 30995507]
5. TCGA. Integrated Genomic Characterization of Pancreatic Ductal Adenocarcinoma. Cancer Cell 2017;32:185–203 e13. [PubMed: 28810144]
6. Lasorella A, Benezra R, Iavarone A. The ID proteins: master regulators of cancer stem cells and tumour aggressiveness. Nat Rev Cancer 2014;14:77–91. [PubMed: 24442143]
7. Winter JM, Tang LH, Klimstra DS, Brennan MF, Brody JR, Rocha FG, et al. A novel survival-based tissue microarray of pancreatic cancer validates MUC1 and mesothelin as biomarkers. PLoS One 2012;7:e40157. [PubMed: 22792233]
8. Bardeesy N, Cheng KH, Berger JH, Chu GC, Pahler J, Olson P, et al. Smad4 is dispensable for normal pancreas development yet critical in progression and tumor biology of pancreas cancer. Genes Dev 2006;20:3130–46. [PubMed: 17114584]
9. GTEx. The Genotype-Tissue Expression (GTEx) project. Nat Genet 2013;45:580–5. [PubMed: 23715323]
10. Bailey P, Chang DK, Nones K, Johns AL, Patch AM, Gingras MC, et al. Genomic analyses identify molecular subtypes of pancreatic cancer. Nature 2016;531:47–52. [PubMed: 26909576]
11. Masui T, Swift GH, Deering T, Shen C, Coats WS, Long Q, et al. Replacement of Rbpj with Rbpjl in the PTF1 complex controls the final maturation of pancreatic acinar cells. Gastroenterology 2010;139:270–80. [PubMed: 20398665]
12. Pin CL, Rukstalis JM, Johnson C, Konieczny SF. The bHLH transcription factor Mist1 is required to maintain exocrine pancreas cell organization and acinar cell identity. J Cell Biol 2001;155:519–30. [PubMed: 11696558]
13. von Figura G, Morris JPt, Wright CV, Hebrok M. Nr5a2 maintains acinar cell differentiation and constrains oncogenic Kras-mediated pancreatic neoplastic initiation. Gut 2014;63:656–64. [PubMed: 23645620]
14. Artner I, Blanchi B, Raum JC, Guo M, Kaneko T, Cordes S, et al. MafB is required for islet beta cell maturation. Proc Natl Acad Sci U S A 2007;104:3853–8. [PubMed: 17360442]
15. Henry C, Close AF, Buteau J. A critical role for the neural zinc factor ST18 in pancreatic beta-cell apoptosis. J Biol Chem 2014;289:8413–9. [PubMed: 24509857]
16. Karlsson O, Thor S, Norberg T, Ohlsson H, Edlund T. Insulin gene enhancer binding protein Isl-1 is a member of a novel class of proteins containing both a homeo- and a Cys-His domain. Nature 1990;344:879–82. [PubMed: 1691825]
17. Sander M, Neubuser A, Kalamaras J, Ee HC, Martin GR, German MS. Genetic analysis reveals that PAX6 is required for normal transcription of pancreatic hormone genes and islet development. Genes Dev 1997;11:1662–73. [PubMed: 9224716]
18. Fusco A, Fedele M. Roles of HMGA proteins in cancer. Nat Rev Cancer 2007;7:899–910. [PubMed: 18004397]
19. Murray IA, Patterson AD, Perdew GH. Aryl hydrocarbon receptor ligands in cancer: friend and foe. Nat Rev Cancer 2014;14:801–14. [PubMed: 25568920]

20. Tetreault MP, Yang Y, Katz JP. Kruppel-like factors in cancer. Nat Rev Cancer 2013;13:701–13. [PubMed: 24060862]
21. Moffitt RA, Marayati R, Flate EL, Volmar KE, Loeza SG, Hoadley KA, et al. Virtual microdissection identifies distinct tumor- and stroma-specific subtypes of pancreatic ductal adenocarcinoma. Nat Genet 2015;47:1168–78. [PubMed: 26343385]
22. Kang Y, Chen CR, Massague J. A self-enabling TGFbeta response coupled to stress signaling: Smad engages stress response factor ATF3 for Id1 repression in epithelial cells. Mol Cell 2003;11:915–26. [PubMed: 12718878]
23. Padua D, Zhang XH, Wang Q, Nadal C, Gerald WL, Gomis RR, et al. TGFbeta primes breast tumors for lung metastasis seeding through angiopoietin-like 4. Cell 2008;133:66–77. [PubMed: 18394990]
24. Anido J, Saez-Borderias A, Gonzalez-Junca A, Rodon L, Folch G, Carmona MA, et al. TGF-beta Receptor Inhibitors Target the CD44(high)/Id1(high) Glioma-Initiating Cell Population in Human Glioblastoma. Cancer Cell 2010;18:655–68. [PubMed: 21156287]
25. Barrett LE, Granot Z, Coker C, Iavarone A, Hambardzumyan D, Holland EC, et al. Self-renewal does not predict tumor growth potential in mouse models of high-grade glioma. Cancer Cell 2012;21:11–24. [PubMed: 22264785]
26. Ischenko I, Petrenko O, Hayman MJ. Analysis of the tumor-initiating and metastatic capacity of PDX1-positive cells from the adult pancreas. Proc Natl Acad Sci U S A 2014;111:3466–71. [PubMed: 24550494]
27. Li C, Heidt DG, Dalerba P, Burant CF, Zhang L, Adsay V, et al. Identification of pancreatic cancer stem cells. Cancer Res 2007;67:1030–7. [PubMed: 17283135]
28. Hermann PC, Huber SL, Herrler T, Aicher A, Ellwart JW, Guba M, et al. Distinct populations of cancer stem cells determine tumor growth and metastatic activity in human pancreatic cancer. Cell Stem Cell 2007;1:313–23. [PubMed: 18371365]
29. Lonardo E, Hermann PC, Mueller MT, Huber S, Balic A, Miranda-Lorenzo I, et al. Nodal/Activin signaling drives self-renewal and tumorigenicity of pancreatic cancer stem cells and provides a target for combined drug therapy. Cell Stem Cell 2011;9:433–46. [PubMed: 22056140]
30. Takeda N, Jain R, LeBoeuf MR, Wang Q, Lu MM, Epstein JA. Interconversion between intestinal stem cell populations in distinct niches. Science 2011;334:1420–4. [PubMed: 22075725]
31. Zhang M, Behbod F, Atkinson RL, Landis MD, Kittrell F, Edwards D, et al. Identification of tumor-initiating cells in a p53-null mouse model of breast cancer. Cancer Res 2008;68:4674–82. [PubMed: 18559513]
32. Ramachandran A, Vizan P, Das D, Chakravarty P, Vogt J, Rogers KW, et al. TGF-beta uses a novel mode of receptor activation to phosphorylate SMAD1/5 and induce epithelial-to-mesenchymal transition. Elife 2018;7:e31756. [PubMed: 29376829]
33. Ahn DH, Li J, Wei L, Doyle A, Marshall JL, Schaaf LJ, et al. Results of an abbreviated phase-II study with the Akt Inhibitor MK-2206 in Patients with Advanced Biliary Cancer. Sci Rep 2015;5:12122. [PubMed: 26161813]
34. Joung J, Konermann S, Gootenberg JS, Abudayyeh OO, Platt RJ, Brigham MD, et al. Genome-scale CRISPR-Cas9 knockout and transcriptional activation screening. Nat Protoc 2017;12:828–63. [PubMed: 28333914]
35. Sanjana NE, Shalem O, Zhang F. Improved vectors and genome-wide libraries for CRISPR screening. Nat Methods 2014;11:783–84. [PubMed: 25075903]
36. Zehir A, Benayed R, Shah RH, Syed A, Middha S, Kim HR, et al. Mutational landscape of metastatic cancer revealed from prospective clinical sequencing of 10,000 patients. Nat Med 2017;23:703–13. [PubMed: 28481359]
37. Kajno E, McGraw TE, Gonzalez E. Development of a new model system to dissect isoform specific Akt signalling in adipocytes. Biochem J 2015;468:425–34. [PubMed: 25856301]
38. Korchynskyi O, ten Dijke P. Identification and functional characterization of distinct critically important bone morphogenetic protein-specific response elements in the Id1 promoter. J Biol Chem 2002;277:4883–91. [PubMed: 11729207]

39. Birkenkamp KU, Essafi A, van der Vos KE, da Costa M, Hui RC, Holstege F, et al. FOXO3a induces differentiation of Bcr-Abl-transformed cells through transcriptional down-regulation of Id1. J Biol Chem 2007;282:2211–20. [PubMed: 17132628]
40. Shi G, Zhu L, Sun Y, Bettencourt R, Damsz B, Hruban RH, et al. Loss of the acinar-restricted transcription factor Mist1 accelerates Kras-induced pancreatic intraepithelial neoplasia. Gastroenterology 2009;136:1368–78. [PubMed: 19249398]
41. Krah NM, De La OJ, Swift GH, Hoang CQ, Willet SG, Chen Pan F, et al. The acinar differentiation determinant PTF1A inhibits initiation of pancreatic ductal adenocarcinoma. Elife 2015;4:e07125.
42. Williams JA, Goldfine ID. The insulin-pancreatic acinar axis. Diabetes 1985;34:980–6. [PubMed: 2412919]
43. Magruder JT, Elahi D, Andersen DK. Diabetes and pancreatic cancer: chicken or egg? Pancreas 2011;40:339–51. [PubMed: 21412116]
44. Li D, Yeung SC, Hassan MM, Konopleva M, Abbruzzese JL. Antidiabetic therapies affect risk of pancreatic cancer. Gastroenterology 2009;137:482–8. [PubMed: 19375425]
45. Hopkins BD, Pauli C, Xing D, Wang DG, Li X, Wu D, et al. Suppression of insulin feedback enhances the efficacy of PI3K inhibitors. Nature 2018;560:499–503. [PubMed: 30051890]
46. Ardito CM, Gruner BM, Takeuchi KK, Lubeseder-Martellato C, Teichmann N, Mazur PK, et al. EGF receptor is required for KRAS-induced pancreatic tumorigenesis. Cancer Cell 2012;22:304–17. [PubMed: 22975374]
47. Navas C, Hernandez-Porras I, Schuhmacher AJ, Sibilia M, Guerra C, Barbacid M. EGF receptor signaling is essential for k-ras oncogene-driven pancreatic ductal adenocarcinoma. Cancer Cell 2012;22:318–30. [PubMed: 22975375]
48. Chaudhary J, Garland W, Salvador R. A novel small molecule inhibitor of Id proteins (AGX-51) blocks cell survival in vitro and diminishes angiogenesis and tumor growth in vivo. The FASEB Journal 2009;23:761.4.
49. Boj SF, Hwang CI, Baker LA, Chio II, Engle DD, Corbo V, et al. Organoid models of human and mouse ductal pancreatic cancer. Cell 2015;160:324–38. [PubMed: 25557080]
50. Jones S, Zhang X, Parsons DW, Lin JC, Leary RJ, Angenendt P, et al. Core signaling pathways in human pancreatic cancers revealed by global genomic analyses. Science 2008;321:1801–6. [PubMed: 18772397]
51. Buenrostro JD, Giresi PG, Zaba LC, Chang HY, Greenleaf WJ. Transposition of native chromatin for fast and sensitive epigenomic profiling of open chromatin, DNA-binding proteins and nucleosome position. Nat Methods 2013;10:1213–8. [PubMed: 24097267]
52. Hahn SA, Schutte M, Hoque AT, Moskaluk CA, da Costa LT, Rozenblum E, et al. DPC4, a candidate tumor suppressor gene at human chromosome 18q21.1. Science 1996;271:350–3. [PubMed: 8553070]

## Significance

Half of pancreatic ductal adenocarcinomas (PDAs) escape TGF-β-induced tumor suppression without inactivating the TGF-β pathway. We report that *ID1* expression is selected for in PDAs and that *ID1* uncouples TGF-β-induced epithelial-to-mesenchymal transition (EMT) from apoptosis. ID1 thus emerges as a crucial regulatory node and a target of interest in PDA.

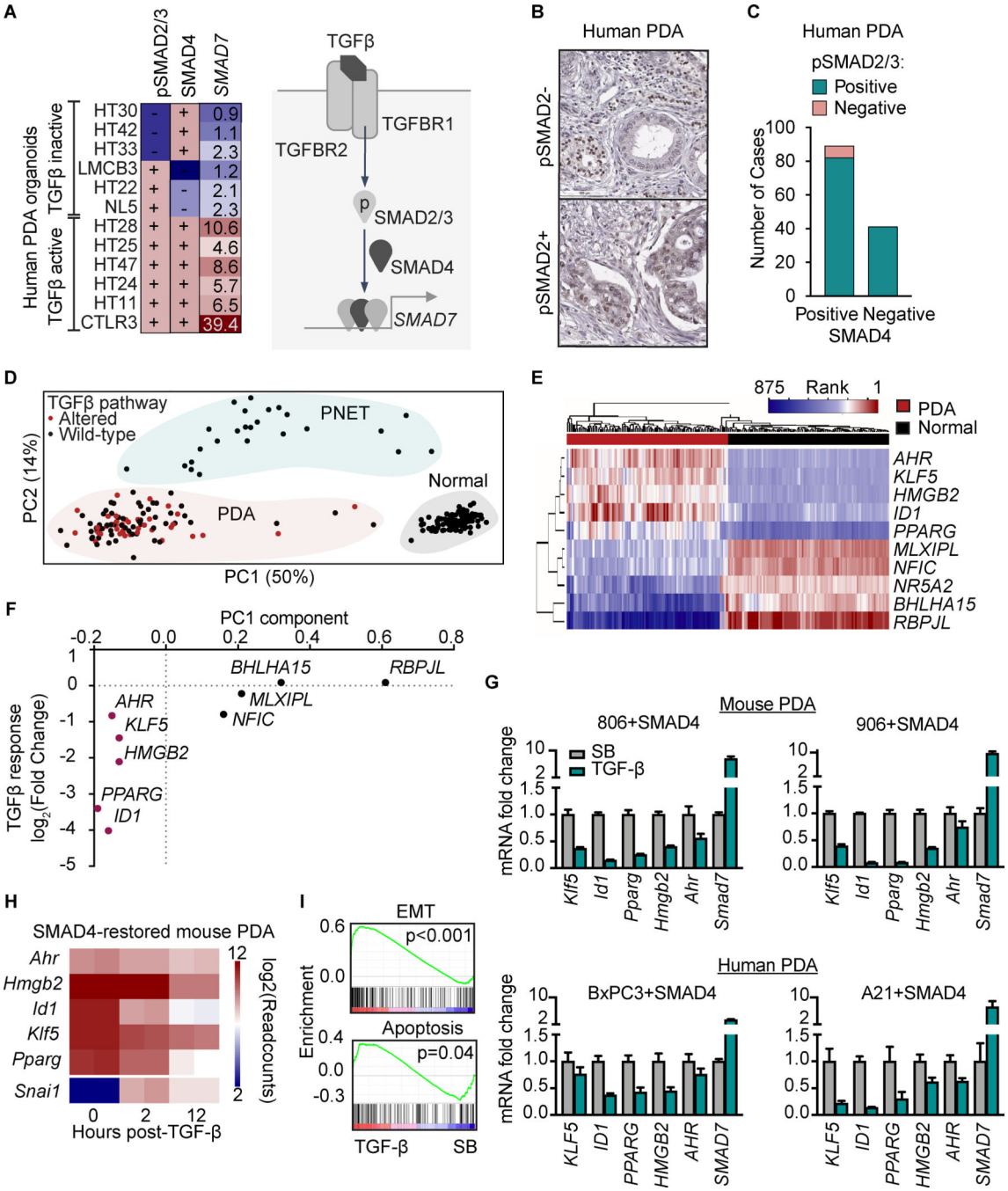


**Figure 1: TGF-β signaling and transcriptional networks in PDA**

A) Human PDA organoids were treated with or without 100 pM TGF-β for 2 h. SMAD4 and pSMAD2 were detected by Western immunoblotting (WB) and *SMAD7* transcript by qRT-PCR. Values reported for *SMAD7* represent fold increase induced by TGF-β. (+), strong band detected by WB; (–), weak or absent band (refer to Supplementary Fig. S1B). A schematic representation of the core TGF-β pathway components and *SMAD7* as a target gene is included.

B-C) A formaldehyde-fixed, paraffin-embedded tissue microarray was constructed of 130 human PDA samples collected at surgical resection and subjected to pSMAD2 and SMAD4 IHC. Samples were scored positive if ≥50% of spots contained pSMAD2 in the tumor cells (B). The number of pSMAD2+ and pSMAD2– cases in the SMAD4+ and SMAD4– groups is plotted (C).

D) RNA-seq datasets of normal pancreas, PDA, and PNET from GTEx and ICGC were curated for transcription factors. Principal component analysis (PCA) was performed of the factors ranked within the top 5 of at least one case. See Supplementary Fig. S1D for complete list of factors included in the PCA. Each dot represents one tumor sample.

E) Using the top 10 PC1 genes from Figure 1D, unsupervised clustering was performed of the rank-based analysis of RNA-seq datasets from GTEx and ICGC. Each column represents one tumor sample.

F) SMAD4-restored $Kras^{G12D}$;$Cdkn2a^{-/-}$;$Smad4^{-/-}$ mouse PDA cells (806 cell line) were treated with 100 pM TGF-β or 2.5 μM SB505124 TGFBRI kinase inhibitor (SB) for 12 h. The samples were subjected to RNA-seq analysis. The fold-change in mRNA levels of the top 10 PC1 genes in TGF-β-treated samples compared to SB-treated samples is shown. Data are averages of two replicates per sample.

G) SMAD4-restored $Kras^{G12D}$;$Cdkn2a^{-/-}$;$Smad4^{-/-}$ mouse PDA cells (806 and 906 cell lines) and SMAD4-restored human BxPC3 and A21 PDA cell lines were treated as in (F) and subjected to qRT-PCR analysis for the indicated genes

H) Heatmap representation of the mRNA levels of the indicated genes in RNA-seq data sets of SMAD4-restored $Kras^{G12D}$;$Cdkn2a^{-/-}$;$Smad4^{-/-}$ mouse PDA cells treated with 100 pM TGF-β for the indicated times. Two replicates per sample.

I) Gene set enrichment analysis (GSEA) of RNA-seq of SMAD4-restored mouse PDA cells treated with 100 pM TGF-β or 2.5 μM SB505124 for 12 h. Two replicates per sample.

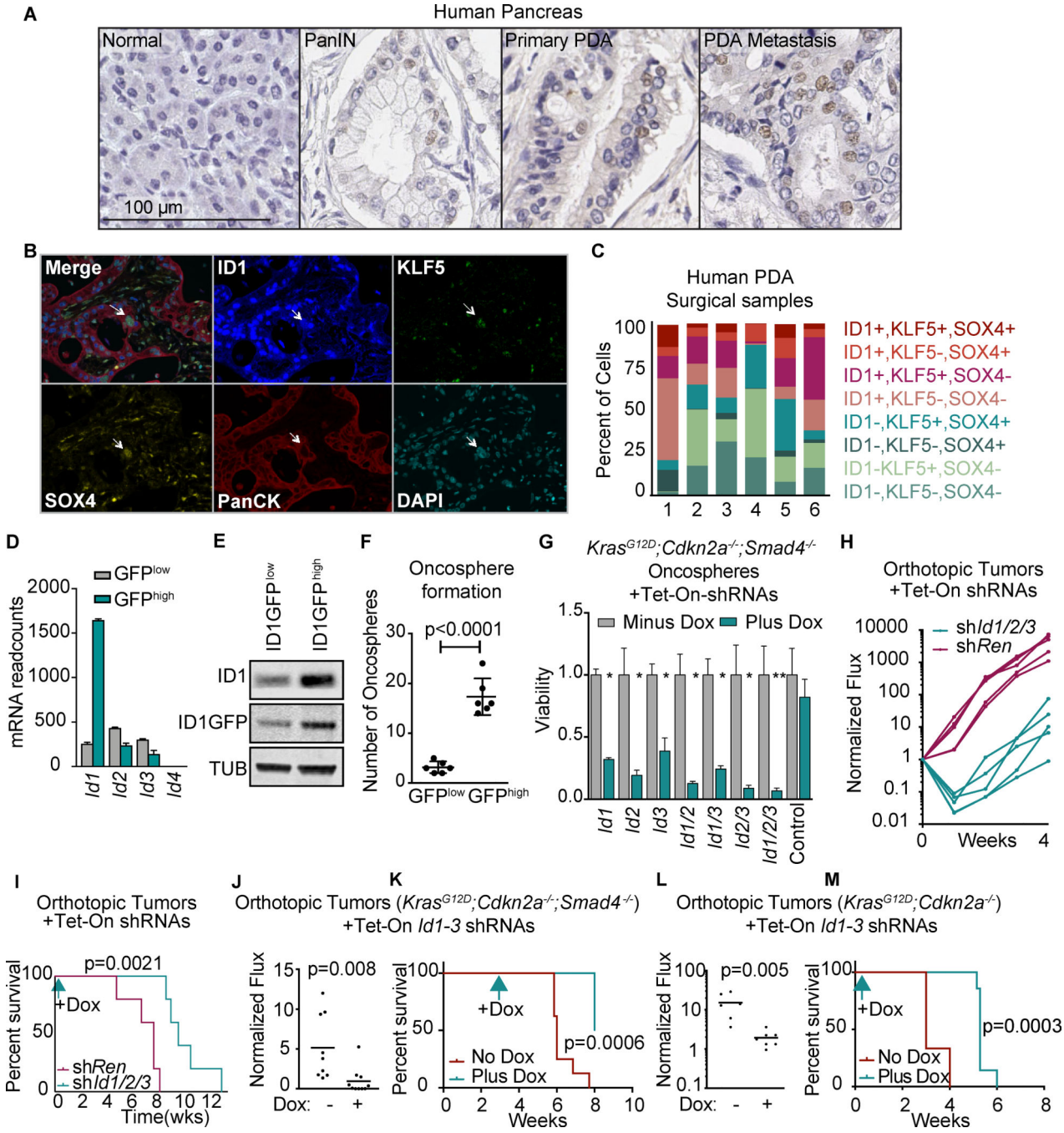


**Figure 2: ID1 expression and effects in PDA progenitors**

A) Representative samples of human normal pancreas, PanIN, primary PDA, and PDA metastasis subjected to ID1 IHC analysis.

B) Four-color multiplex IHC staining for ID1, KLF5, SOX4, and pan-cytokeratins in surgical PDA samples. *Arrow*, an ID1+,KLF5+,SOX4+ epithelial cell.

C) Quantification of ID1, KLF5, and SOX4 expressing cancer cells in six surgical PDA samples (refer to Supplementary Table S1).

D) *Id1*, *Id2* and *Id3* mRNA levels in sorted ID1-GFP$^{high}$ and ID1-GFP$^{low}$ mouse PDA cells detected by RNA-seq.

E) ID1 and ID1-GFP levels in sorted ID1-GFP$^{high}$ and ID1-GFP$^{low}$ mouse PDA cells.

F) *Kras*$^{G12D}$;*Cdkn2a*$^{-/-}$;*Smad4*$^{-/-}$ mouse PDA cells were engineered to express an ID1-GFP endogenous reporter (Supplementary Fig. S2E) and sorted based on GFP expression (Supplementary Fig. S2F). Cells were subjected to spheroid growth assays by plating 500 cells/well in low-adhesion 96-well plates, grown for 1 week, and spheroid colonies were counted. n=6 per group. Unless otherwise noted, p-values and statistics were calculated by unpaired, two-sided t-test, alpha = 0.05, as described in the Methods section.

G) *Kras*$^{G12D}$;*Cdkn2a*$^{-/-}$;*Smad4*$^{-/-}$ mouse PDA cells were engineered with doxycycline-inducible (Tet-ON) shRNAs targeting *Id* genes singly or in the indicated combinations, and subjected to spheroid growth assays with or without doxycycline. Cell viability was measured by CellTiter-Glo 5 days after doxycycline addition. n=3 per group, mean ±SD, all comparisons against control. * $p<0.01$, ** $p<0.001$.

H,I) *Kras*$^{G12D}$;*Cdkn2a*$^{-/-}$;*Smad4*$^{-/-}$ mouse PDA cells with Tet-ON shRNAs targeting *Id1, Id2,* and *Id3* or a control shRNA (*shRen*) were orthotopically implanted at 500 cells per pancreas. Mice were started on doxycycline diet 3 days after implantation. (H) BLI (photon flux) was measured weekly. (I) Survival analysis. n=5 per group, p-value calculated by log-rank test.

J,K) *Kras*$^{G12D}$;*Cdkn2a*$^{-/-}$;*Smad4*$^{-/-}$ mouse PDA cells with Tet-On shRNAs targeting *Id1, Id2,* and *Id3* were orthotopically implanted at 500 cells per pancreas. Three weeks later, mice were randomized to matched bioluminescent groups and one group was started on doxycycline diet. n=10 per group. p-values calculated by unpaired two-sided t-test (J), and log-rank test (K).

L,M) *Kras*$^{G12D}$;*Cdkn2a*$^{-/-}$ mouse PDA cells with Tet-On shRNAs targeting *Id1–3* were orthotopically implanted at 500 cells per pancreas. Three days after implantation, one group was started on doxycycline diet. Bioluminescent reading at 1 week post-implantation. n=6–7 per group, p-values calculated by unpaired two-sided t-test (L), and log-rank test (M)

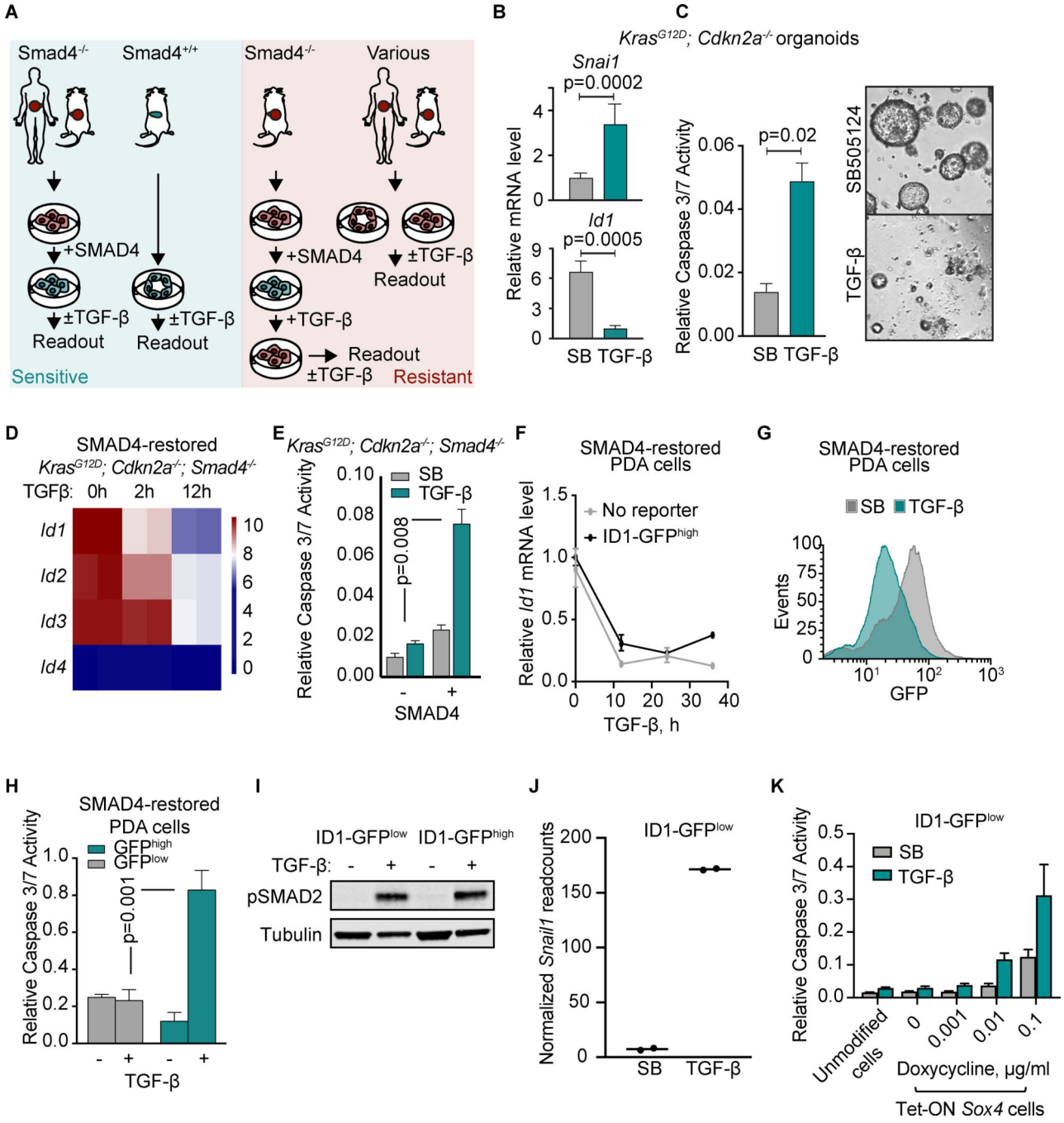


**Figure 3: ID1 downregulation is associated with apoptosis**

A) Human and mouse PDA-derived cell models to recapitulate states that are sensitive or resistant to TGF-β-mediated apoptosis.

B) qRT-PCR analysis of *Id1* and *Snai1* mRNA levels in $Kras^{G12D}$;$Cdkn2a^{-/-}$ mouse organoids treated with 2.5 μM SB505124 (SB) or 100 pM TGF-β for 2h. Mean ±range of 3 replicates, representative of two independent experiments.

C) Apoptosis measured by CaspaseGlo 3/7 36 h after treatment with TGF-β or SB. Two-tailed, unpaired t-test. Mean±SD of 3 replicates, representative of two independent experiments. *Right*, cell viability visualized by microscopy 4 days after treatment.
D) *Id* mRNA levels from RNA-seq analysis of SMAD4-restored mouse *Kras*$^{G12D}$;*Cdkn2a*$^{-/-}$;*Smad4*$^{-/-}$ PDA cells treated with 100 pM TGF-β for the indicated times.
E) *Kras*$^{G12D}$;*Cdkn2a*$^{-/-}$;*Smad4*$^{-/-}$ mouse PDA cells with and without SMAD4 restoration were treated with SB or TGF-β for 36 h. Apoptosis was measured by CaspaseGlo 3/7. Mean ±SD of 3 replicates, representative of two experiments.
F) qRT-PCR for *Id1* in SMAD4-restored mouse PDA cells with and without the ID1-GFP reporter. Mean±range of 3 replicates, representative of two independent experiments.
G) Flow cytometry analysis of GFP expression of SMAD4-restored mouse PDA cells with the ID1-GFP reporter and treated with SB or TGF-β for 36h.
H) SMAD4-restored mouse PDA cells with the ID1-GFP reporter were sorted for GFP expression and then treated with 2.5 μM SB or 100 pM TGF-β for 36h. Apoptosis was measured by CaspaseGlo 3/7. Mean ±SD of 3 replicates, representative of two experiments.
I) Phospho-SMAD2 levels in ID1-GFP$^{low}$ and ID1-GFP$^{high}$ cells treated with SB or TGF-β for 2h.
J) qRT-PCR analysis of *Snai1* transcript levels in in ID1-GFP$^{low}$ and ID1-GFP$^{high}$ cells treated with SB or TGF-β for 2h.
K) SMAD4-restored mouse PDA cells with the ID1-GFP reporter were transduced with a Tet-On *Sox4* vector, sorted for low GFP expression and treated with the indicated concentrations of doxycycline for 12h, then 2.5 μM SB or 100 pM TGF-β were added for 36h. Apoptosis was measured by CaspaseGlo 3/7. Mean ±SD of 5 replicates, representative of two experiments, two-tailed unpaired t-tests.

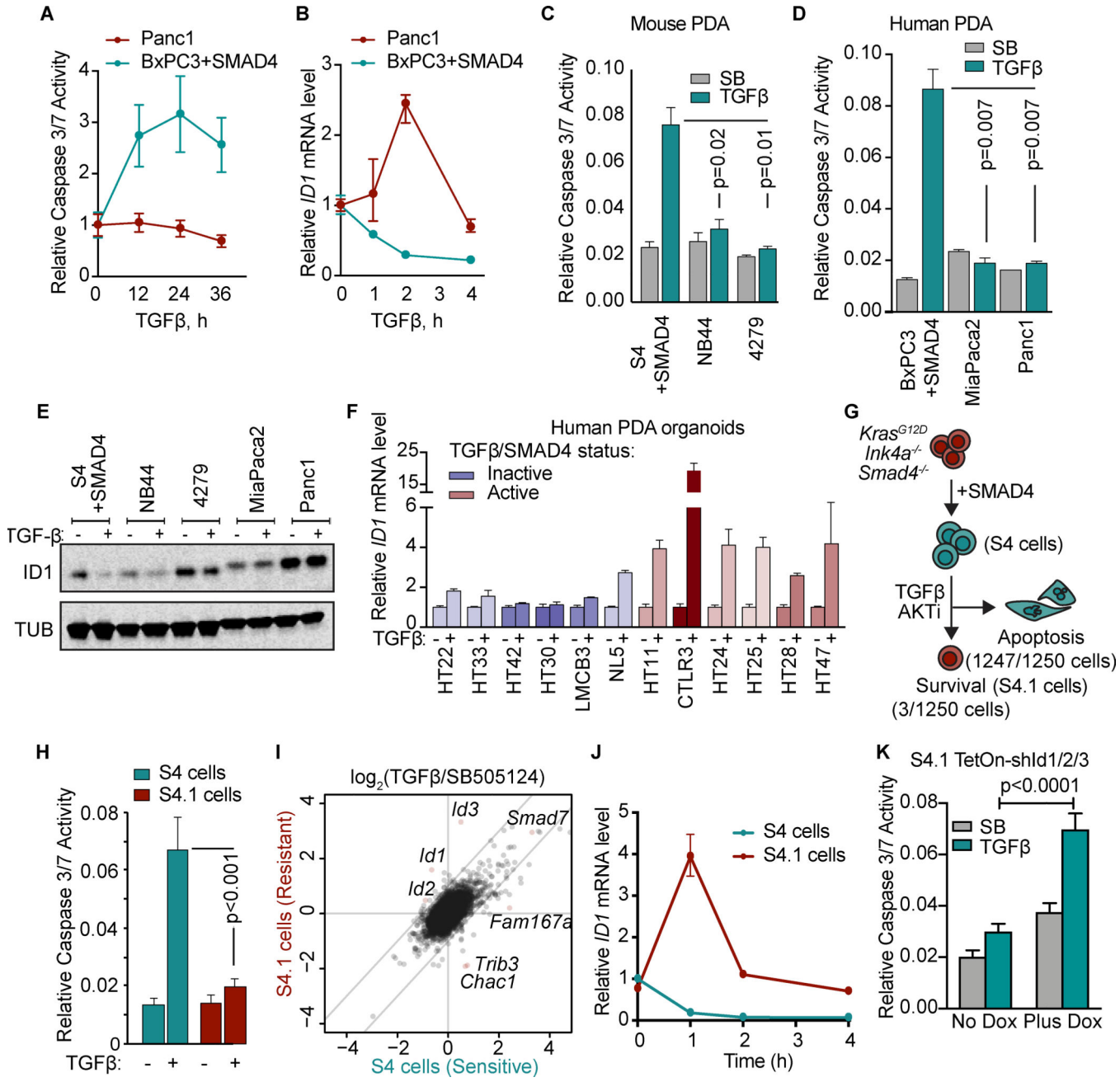


**Figure 4: Dysregulated ID1 expression in PDAs with a functional TGF-β pathway**

A,B) Human PDA cell lines with wild type SMAD4 (Panc1) or with restored SMAD4 (BxPC3+SMAD4) were treated with 100 pM TGF-β for the indicated times. Apoptosis was measured by CaspaseGlo 3/7 and *ID1* mRNA levels by qRT-PCR.

C) SMAD4-restored *Kras*$^{G12D}$;*Cdkn2a*$^{-/-}$;*Smad4*$^{-/-}$ mouse PDA cells (S4), and two *Kras*$^{G12D}$;*Cdkn2a*$^{-/-}$ mouse PDA cell lines with wild type SMAD4 (NB44 and 4279) were treated with 2.5 μM SB505124 or 100 pM TGF-β for 36 h. Apoptosis was determined using CaspaseGlo 3/7. Mean ±SD, n=2, two-tailed unpaired t-tests.

D) SMAD4-restored BxPC3 human PDA cells, and the SMAD4 wild type MiaPaca2 and Panc1 human PDA cell lines were treated with 2.5 μM SB505124 or 100 pM TGF-β for 36h and assayed using CaspaseGlo 3/7 and CellTiter-Glo. Mean±SD, n=2, two-tailed unpaired t-tests.

E) S4, NB44, 4279, MiaPaca2, and Panc1 cells were treated with 2.5 μM SB505124 or 100 pM TGF-β for 24 h and subjected to ID1 and tubulin immunoblotting analysis.

F) qRT-PCR analysis of *ID1* mRNA levels in human PDA organoids treated with or without TGF-β for 2 h. Mean±range of 3 replicates.

G) SMAD4-restored $Kras^{G12D}$;$Cdkn2a^{-/-}$;$Smad4^{-/-}$ mouse PDA cells were treated with 100 pM TGF-β and 2.5 μM MK2206 AKT inhibitor for 3 weeks, and surviving cells were selected.

H) SMAD4-restored $Kras^{G12D}$;$Cdkn2a^{-/-}$;$Smad4^{-/-}$ mouse PDA cells (S4) and a resistant population selected as described in G (S4.1 cells) were treated with 2.5 μM SB or 100 pM TGF-β, in the presence of 2.5 μM MK2206, for 36 h. Apoptosis was measured using CaspaseGlo 3/7. n=6 per group, mean ±SD.

I) S4 and S4.1 cells were treated with 2.5 μM SB or 100 pM TGF-β, in the presence of 2.5 μM MK2206, for 1.5h and subjected to RNA-seq analysis. Two replicates per sample.

J) S4 and S4.1 cells were treated with 100 pM TGF-β for the indicated times and *Id1* mRNA level was determined by qRT-PCR. Mean±range of 3 replicates, representative of 2 independent experiments.

K) S4.1 cells with Tet-On shRNAs targeting *Id1–3* were treated with 2.5 μM SB or 100 pM TGF-β, in the presence of 2.5 μM MK2206, for 36 h. Apoptosis was measured using CaspaseGlo 3/7. n=5 per group, mean ±SD, two-tailed unpaired t-test.

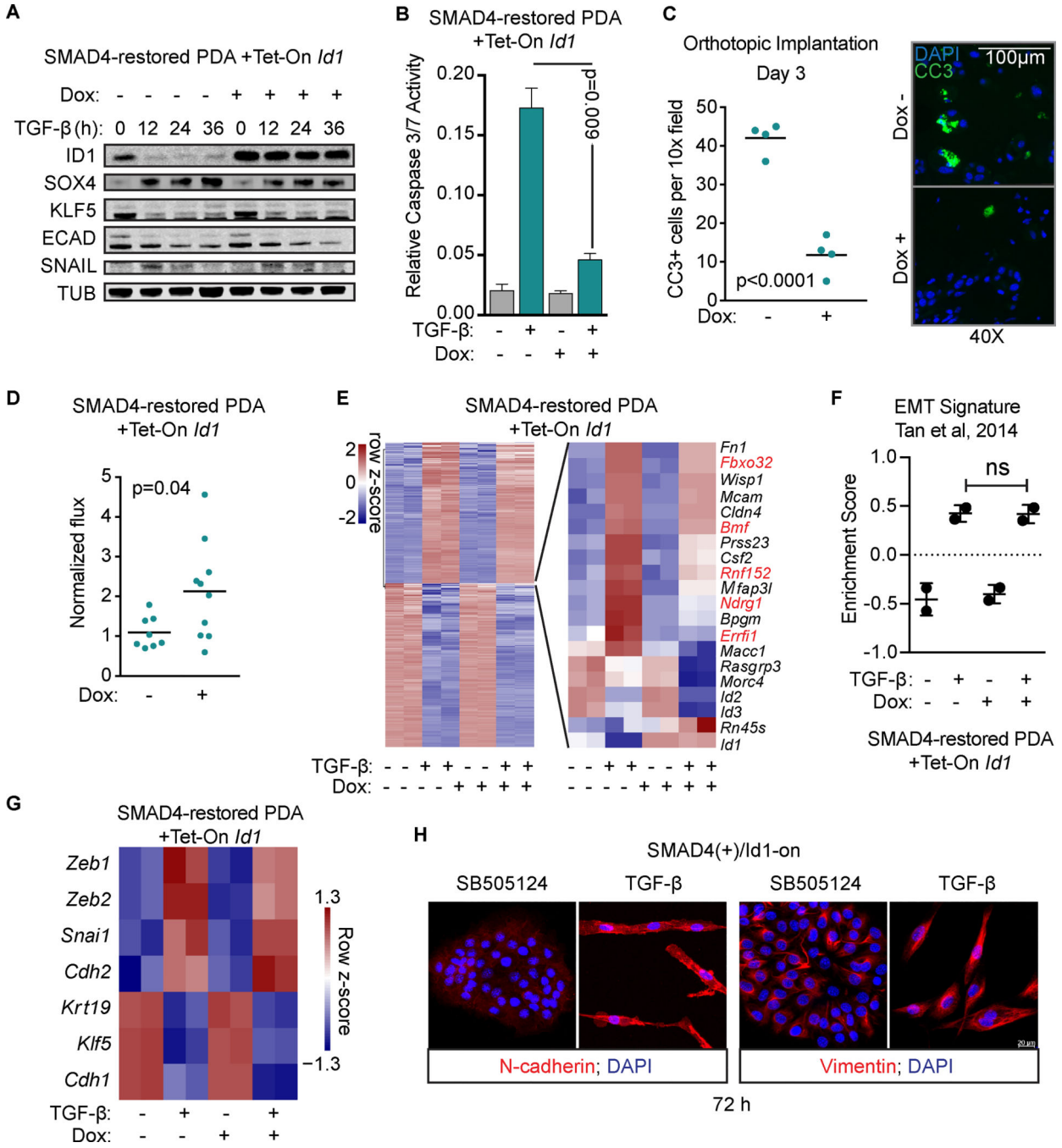


**Figure 5: ID1 uncouples TGF-β-induced EMT from apoptosis**

A) SMAD4-restored *Kras*$^{G12D}$;*Cdkn2a*$^{-/-}$;*Smad4*$^{-/-}$ mouse PDA cells transduced with a Tet-On *Id1* construct were treated as indicated and subjected to immunoblotting analysis for the indicated proteins. *ECAD,* E-cadherin.

B) The SMAD4-restored Tet-On *Id1* mouse PDA cells described in (A) were incubated with or without doxycycline for 12 h and then with 2.5 μM SB505124 or 100 pM TGF-β for 36h. Apoptosis was assayed using CaspaseGlo 3/7. n=2, mean ±SD.

C) The SMAD4-restored Tet-On *Id1* mouse PDA cells described in (A) were treated with doxycycline for 1 day and orthotopically implanted into mice with caerulein-induced pancreatitis. Pancreata were collect at 72h for immunofluorescence analysis of cleaved caspase-3 positive (CC3+) cells. Two-tailed unpaired t-test, n=4 mice per group.
D) The SMAD4-restored Tet-On *Id1* mouse PDA cells described in (A) were transduced with a luciferase construct and implanted into the pancreata of mice with caerulein-induced pancreatitis. BLI was measured at 1 week. Two-tailed unpaired t-test, n=8–10 mice per group.
E) The SMAD4-restored Tet-On *Id1* mouse PDA cells described in (A) were treated with or without doxycycline for 12 h and then with 2.5 μM SB505124 or 100 pM TGF-β for 24h. Two replicates per sample we subjected to RNA-seq. Differentially expressed genes in response to TGF-β are represented as a heatmap on the left. The right inset shows genes that were differentially regulated ±doxycycline.
F) EMT gene set variation analysis of RNA-seq dataset in *E.* n=2, mean±SD.
G) TGF-β effects on EMT-related gene expression in the RNA-seq dataset in *E.*
H) Cells were treated as in B for 72h and subjected to inmunofluorescence staining for the EMT mesenchymal markers N-cadherin and vimentin.

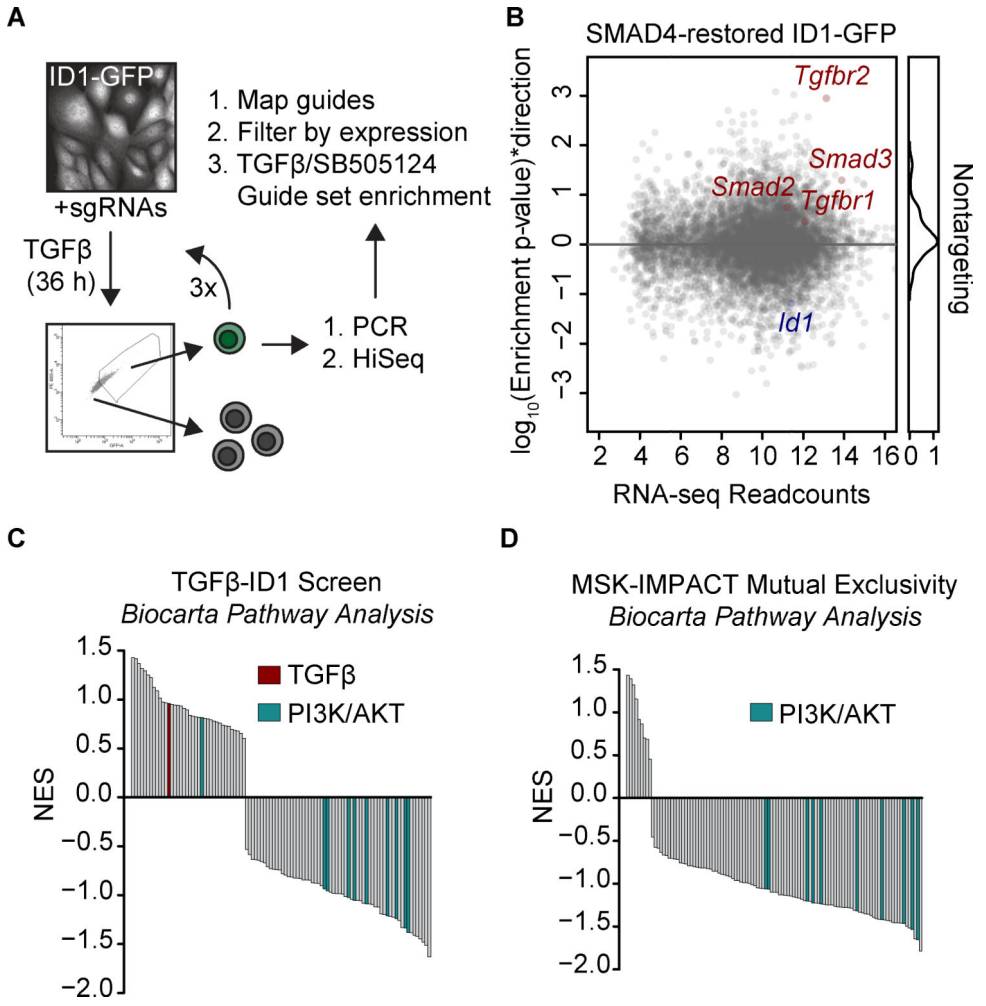


**Figure 6: Mediators of ID1 dysregulation in PDA**

A) Scheme of a CRISPR/Cas9 screen for mediators of ID1 dysregulation in PDA. SMAD4-restored mouse PDA cells expressing an endogenous ID1-GFP reporter and Cas9 were transduced with the Gecko_v2 genome-wide sgRNA library, selected in puromycin for 1 week, and treated for 36 h with 2.5 μM SB505124 or 100 pM TGF-β. ID1-GFP$^{high}$ cells were sorted and the process was repeated 3 times. Cells were collected for analysis of sgDNA sequences.

B) sgRNAs were mapped and sgRNAs targeting genes expressed in PDA cells were selected. Gene enrichment in the TGF-β vs SB505124 samples was determined using the CAMERA competitive gene set test. Y-axis was calculated as p-value * (±1), where +1=enriched and −1=depleted. n=2 per group.

C) Genes enriched in the genome-wide screen were ranked by (direction * p-value) and gene set enrichment analysis of Biocarta pathways was performed.

D) MSK-IMPACT mutations mutually exclusive to TGF-β pathway alterations were analyzed via cBioPortal and ranked by $-\log_{10}$(p-value) for mutual exclusivity. Gene set enrichment analysis of Biocarta pathways was performed.

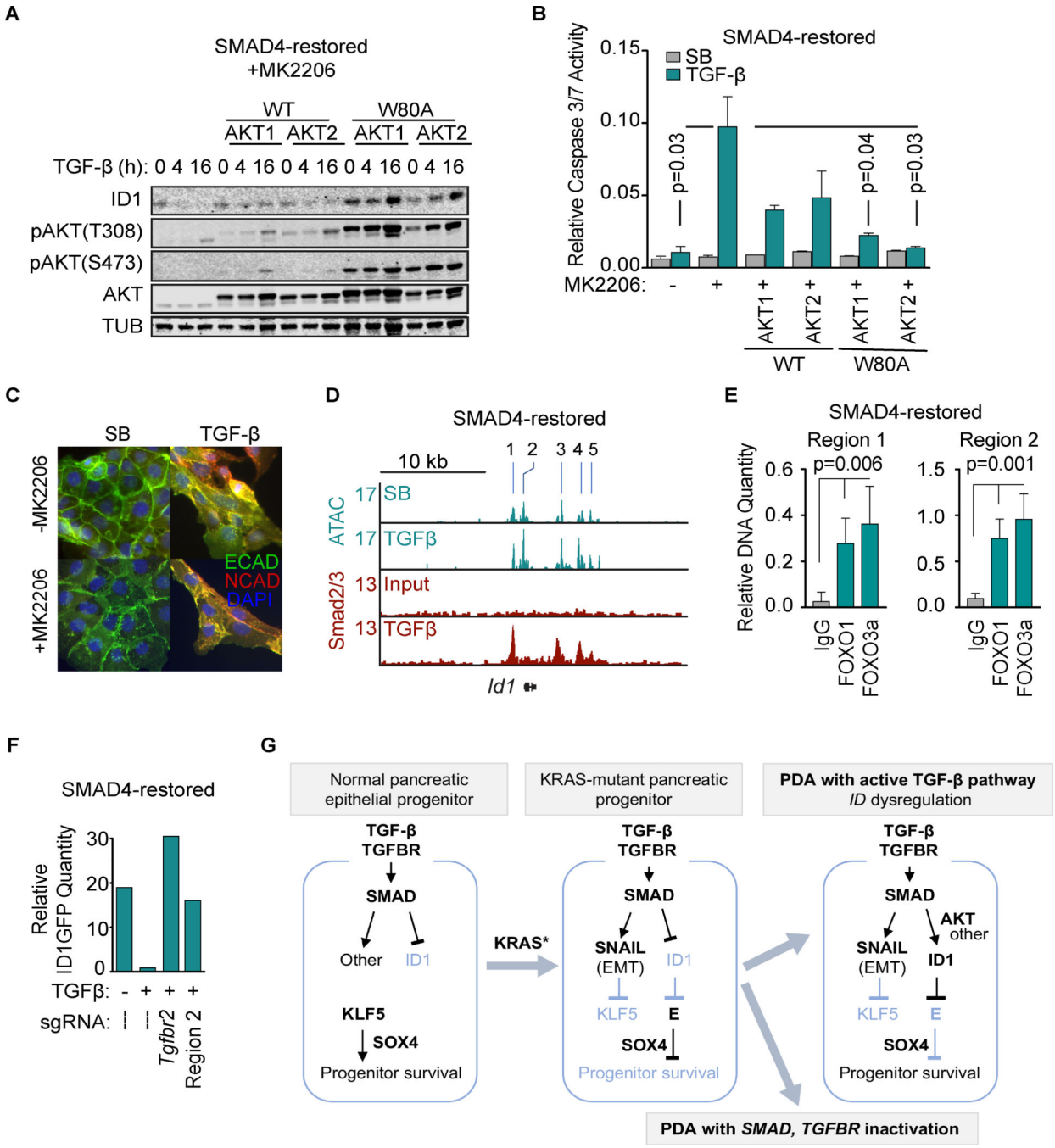


**Figure 7: Mechanisms for loss of ID1 repression in PDA**

A) SMAD4-restored mouse PDA cells were transduced with wild type or MK2206-resistant (W80A) mutant forms of AKT1 or AKT2, and treated with 2.5 μM MK2206 and 100 pM TGF-β for the indicated times. Samples were subjected to immunoblotting analysis for ID1, AKT, AKT with activating phosphorylations, or tubulin (TUB) as a loading control.

B) SMAD4-restored mouse PDA cells transduced with the indicated AKT constructs were treated with or without 2.5 μM MK2206, and 2.5 μM SB505124 or 100 pM TGF-β for 36 h. Apoptosis was determined by CaspaseGlo 3/7. Two-tailed unpaired t-test, n=2 per group.

C) SMAD4-restored mouse PDA cells were treated with vehicle (DMSO) or 2.5 μM MK2206 for 12h and 2.5 μM SB505124 or 100 pM TGF-β for 28h. E-cadherin and N-cadherin were detected by immunofluorescence.

D) SMAD4-restored mouse PDA cells were treated with 2.5 μM SB505124 or 100 pM TGF-β for 1.5 h and subjected to ATAC-seq and SMAD2/3 ChIP-seq. Gene tracks show ATAC and SMAD2/3 ChIP tags at the *Id1* locus (refer to Figure S7B for additional details)

E) SMAD4-restored mouse PDA cells were treated with 2.5 μM MK2206 for 12h and then 100 pM TGF-β for 1.5h. Samples were subjected to ChIP-PCR analysis of FOXO1 and FOXO3a binding to regions 1 and 2 of the *Id1* locus. Mean ±SD, two-tailed unpaired t-tests.

F) SMAD4-restored mouse PDA cells expressing an endogenous ID1-GFP reporter and Cas9 were transduced with the indicated sgRNAs, treated with 2.5 μM MK2206 for 12h and then with 2.5 μM SB505124 or 100 pM TGF-β for 36h, and analyzed for GFP levels by flow cytometry. Representative of 3 independent experiments.

G) Model of the role of ID1 in TGF-β tumor suppression and PDA progression. Previous work showed that KLF5 and SOX4 co-enforce of a pancreatic epithelial progenitor state and survival, whereas pancreatic progenitors harboring KRAS mutations respond to TGF-β with activation of the master EMT transcription factor SNAIL, which represses KLF5 expression. This KLF5-depleted context activates pro-apoptotic genes (3). Approximately 50% of human PDA tumors progress with inactivation of the TGF-β pathway, owing to genetic inactivation of *SMAD4* and, less frequently, other core components of the TGF-β pathway (5,52). The present results identify dysregulation of ID1 as a basis for progression of the other 50% of human PDA tumors. In tumors that retain an active TGF-β pathway, activation of AKT or various low-frequency genetic alterations switch *ID1* regulation by TGF-β from repression into induction. ID1 inhibits the activation of E12/E47 (E) dependent pro-apoptotic genes, thus decoupling EMT from apoptosis and allowing PDA cells to survive while retaining the ability to undergo EMT.